Susceptibility-weighted imaging at 7 T: Improved diagnosis of cerebral cavernous malformations and associated developmental venous anomalies [☆],[☆☆]

Josa M. Frischer [a],[*], Sabine Göd [b], Andreas Gruber [a], Walter Saringer [a], Günther Grabner [b], Brigitte Gatterbauer [a], Klaus Kitz [a], Sabrina Holzer [a], Claudia Kronnerwetter [b], Johannes A. Hainfellner [c], Engelbert Knosp [a], Siegfried Trattnig [b],[**]

[a] Medical University Vienna, Department of Neurosurgery, Vienna, Austria
[b] Medical University Vienna, Department of Radiology, MR Centre of Excellence, Vienna, Austria
[c] Medical University Vienna, Institute of Neurology, Vienna, Austria

ARTICLE INFO

ABSTRACT

Background and aim: In the diagnosis of cerebral cavernous malformations (CCMs) magnetic resonance imaging is established as the gold standard. Conventional MRI techniques have their drawbacks in the diagnosis of CCMs and associated venous malformations (DVAs). The aim of our study was to evaluate susceptibility weighted imaging SWI for the detection of CCM and associated DVAs at 7 T in comparison with 3 T.
Patients and methods: 24 patients (14 female, 10 male; median age: 38.3 y (21.1 y–69.1 y) were included in the study. Patients enrolled in the study received a 3 T and a 7 T MRI on the same day. The following sequences were applied on both field strengths: a T1 weighted 3D GRE sequence (MP-RAGE) and a SWI sequence. After obtaining the study MRIs, eleven patients underwent surgery and 13 patients were followed conservatively or were treated radio-surgically.
Results: Patients initially presented with haemorrhage (n = 4, 16.7%), seizures (n = 2, 8.3%) or other neurology (n = 18, 75.0%). For surgical resected lesions histopathological findings verified the diagnosis of CCMs. A significantly higher number of CCMs was diagnosed at 7 T SWI sequences compared with 3 T SWI (p < 0.05). Additionally diagnosed lesions on 7 T MRI were significantly smaller compared to the initial lesions on 3 T MRIs (p < 0.001). Further, more associated DVAs were diagnosed at 7 T MRI compared to 3 T MRI.
Conclusion: SWI sequences at ultra-high-field MRI improve the diagnosis of CCMs and associated DVAs and therefore add important pre-operative information.

1. Introduction

Cerebral cavernous malformations (CCM) are a heterogeneous group of lesions mostly described as a mulberry like assembly of vascular sinusoids with varying vessel diameter and wall thickness, lined by a thin endothelium lacking smooth muscle and elastin, surrounded by hemosiderin deposits and gliosis (Frischer et al., 2008; Raychaudhuri et al., 2005).

In the diagnosis of CCM magnetic resonance imaging has proven to be the gold standard. However, conventional MRI techniques also have their drawbacks. If CCM lesions are intact and have not bled, they may be almost invisible except for a faint or ill-defined non-specific blush of enhancement after contrast administration. In addition, the lack of flow-related signal intensity makes CCMs undetectable on conventional MR angiographic techniques (Bertalanffy et al., 2002; Tsui et al., 2009).

It is of further importance that according to the pertinent literature an average of 13–30% of cavernomas are associated with venous malformations (Bertalanffy et al., 2002; Porter et al., 1999). However, several studies showed that the prevalence of cavernomas associated with DVAs is underestimated using routine MRI and that small venous malformations are only diagnosed during surgery (Bertalanffy et al., 2002; Kamezawa et al., 2005; Porter et al., 1999; Wurm et al., 2007). Moreover, it has been described that CCMs with associated venous anomalies present with a higher risk of clinically significant

haemorrhage (Bertalanffy et al., 2002; Porter et al., 1999; Wurm et al., 2007).

The field of magnetic resonance imaging has experienced huge developments in recent years. This especially holds true for a technique formerly known as MR venography. Susceptibility-weighted imaging sequences are highly sensitive for paramagnetic blood degradation products such as desoxyhemoglobin and hemosiderin and enable the exact visualisation even of small vessels. In contrast to conventional MRI sequences that rely on the reading of magnitude information, SWI uses additional phase data. In summary, susceptibility-weighted imaging is a high-spatial resolution, three-dimensional, gradient-echo technique. SWI offers information about any tissue that has a different susceptibility than its surrounding structures such as deoxygenated blood, hemosiderin, ferritin, and calcium. The higher the magnetic field, the higher this susceptibility effect and thus the better the SWI image of e.g. small cerebral white matter veins. This is caused by a higher sensitivity for phase effects, a higher signal to noise ratio and a higher resolution (Haacke et al., 2004, 2009; Ladd, 2007; Mittal et al., 2009).

How or if those effects on ultra-high-field imaging improve the diagnosis of various cerebral pathologies has yet to be evaluated. Few recent studies provide initial data that ultra-high-field magnetic resonance imaging at 7 T improves the detection of cerebral cavernous malformations when compared to 1.5 T (Dammann et al., 2010; Novak et al., 2003; Schlamann et al., 2010). Our study therefore aims to evaluate SWI sequences at 7 T for the detection of CCM and associated DVAs in comparison with SWI at 3 T for the first time in a larger series of CCM patients.

2. Patients and methods

2.1. Sample characterisation and ethical approval

Before commencement of the study, ethical approval was granted by the ethics commission of the Medical University of Vienna. All patients admitted to the Department of Neurosurgery of the Medical University of Vienna between March 2010 and June 2011 with the diagnosis of a cerebral cavernous malformation on the initial routine MRI were screened for this study. Patients therefore presented with lesions on their initial routine MRIs resembling popcorn like structures and were hypointense on T2 weighted images and negative on MR-angiography. Signs of intra- or extralesional haemorrhages (hyperintense on T2 weighted and T1 weighted imaging if in the subacute stage) were additionally observed. Inclusion criteria were applied as follows: no prior therapy of the lesions, above 18 years of age, exclusion of pregnancy, exclusion of an allergy to the contrast medium, exclusion of further contraindications for MRI (cardiac pacemaker, metallic cardiac valves, surgical clips, implanted electrical infusion pump, tattoos, piercing, etc.), normal current creatinine level (prevention of nephrogenic systemic fibrosis), exclusion of claustrophobia.

Clinical data were recorded accordingly: age, sex, presenting symptoms, localisation of initial diagnostic lesion(s). After informed consent patients underwent their 3 T and 7 T study MRIs on the same day. Twenty-four patients (14 female, 10 male) with a median age of 38.3 years (21.1 y–69.1 y) were thus included in the study. After obtaining the study MRIs, patients were treated according to the state of the art treatment plan of the Department of Neurosurgery. Thus, 11 patients underwent surgery of their clinically significant lesions, 12 patients were followed conservatively and 1 patient underwent radio-surgery. For all surgical patients the diagnosis of a CCM could be proven histo-pathologically.

2.2. MRI specifics

Routine MRI sequences were a heterogeneous group of 1.5 T and 3 T sequences but in all cases including T2 weighted sequences and T1 weighted sequences with and without contrast enhancement. Still, the routine MRI sequences were only used to include patients in the presented study. In order to directly compare SWI at 3 T and at 7 T for the detection of CCMs, patients were evaluated with our standardised study protocol. Patients underwent a 3 T and a 7 T MRI on the same day. All patients were examined on a 7 T system (Magnetom, Siemens, Erlangen, Germany) using a 32 channel RF coil (Nova Medical, Wilmington, USA). T1-weighted data were acquired using an MP-RAGE sequence. Afterwards a three-dimensional, fully first-order flow-compensated gradient-echo SWI sequence was performed. The same protocol including an MP-RAGE and SWI was performed on a 3 T MR system (Tim Trio, Siemens, Erlangen, Germany). For detailed MR sequence parameters see Table 1.

2.3. Data evaluation

MRI evaluation was performed by a senior radiologist (S.T.) and a junior radiologist (S.G.) in consensus blinded to clinical and initial diagnostic data as has been described before (Pinker et al., 2007). A third co-worker entered the data into the clinical database (J.M.F.). The number of detected lesions on 3 T and 7 T SWI sequences as stated above was recorded. Additionally, the diagnosis of associated venous anomalies was made. Lesion specifics such as localisation and volume were also recorded. For all patients of the surgical group the diagnosis of a CCM could be proven histo-pathologically. The diagnosis of associated venous malformations was also evaluated intraoperatively for all patients of the surgical group. Artefacts on 7 T scans were rated accordingly: none/minor, present but evaluation possible, major evaluation hardly possible. Lesion volume was evaluated on 7 T scans for all lesions in order to enable comparison of lesions. Lesion volume was calculated by using the following formula: $A \times B \times C / 2$. (A) is the largest diameter and (B) is the perpendicular diameter of lesion. (C) was obtained by summing up the thicknesses of the slices where the lesion was visible (Pantano et al., 1999).

2.4. Statistical analysis

The presented study was prospectively designed. A prospective cohort study, more accurate a comparative study (3 T vs. 7 T) was applied. Due to the grouping of patients after the state of the art treatment plan, the study was not randomised. Patients' data were administered in an anonymous database. Due to the uneven distribution of our data, statistical analysis was performed with nonparametric tests. Descriptive analysis included median value and range as well as number and percentage. Statistical calculations included Wilcoxon test and McNemar test for paired samples as well as Mann–Whitney test. p-Values<0.05 were considered statistically significant. SPSS

Table 1
MRI specifics.

	7 T	3 T
T1 MP-RAGE:		
Image matrix	320×320	320×308
Resolution	0.7 mm isotropic	0.8 mm isotropic
Slices	208	192
Parallel imaging factor	2	2
TR/TI/TE	3800/1700/3.55 ms	2190/1300/3.02 ms
Acquisition time	7:30 min	11:16 min
SWI sequence:		
TE	15 ms	29 ms
TR	28 ms	42 ms
Image-matrix	704×704 pixels	384×384 pixels
Slices	96	88
Parallel imaging factor	2	2
Acquisition time	10.18 min	11:03 min
Resolution	0.3×0.3×1.2 mm	0.6×0.6×1.5 mm

Table 1 shows detailed MRI specifics for the 7 T and 3 T study images.

17.0 statistical software system (SPSS Inc., Chicago, IL) was used for data administration and statistical calculations.

3. Results

The majority (n = 18, 75.0%) of patients initially presented with minor neurological symptoms. Remaining patients presented with haemorrhage (n = 4, 16.7%) and seizures (n = 2, 8.3%). The majority of patients (n = 19, 79.1%) showed single, supratentorial or single infratentorial (n = 3, 12.5%) lesions. Only 2 patients (8.3%) were diagnosed with multiple lesions on their initial routine MRI. All 24 patients included in this study tolerated the MRI examinations well. Artefacts on 7 T MRI scans were none/minor (n = 12, 50.0%) or present but evaluation possible (n = 10, 41.7%) in the majority of patients. In two patients (8.3%) artefacts severely interfered with the evaluation.

Initial routine MRIs were a group of heterogeneous MR protocols but in all cases included T2 weighted MR sequences. In most of the cases contrast enhanced sequences were available. All lesions on the initial routine MRI were also identified on the 3 T and 7 T study examinations. As shown in Fig. 1A, significantly more lesions were detected on 7 T scans (p<0.05) compared to 3 T scans. Thus, six additional patients were diagnosed with multiple lesions. However, lesion size of those additional detected lesions on 7 T MRI sequences was significantly smaller when compared to the initially diagnosed lesions that were already diagnosed on 3 T sequences (p<0.001) (Fig. 1B). Median volume of initial diagnosed lesions was 0.9 cm^3 (0.1–17.5 cm^3). Median volume of additionally diagnosed lesions on 7 T SWI sequences only reached 0.01 cm^3 (0.01 to 0.1 cm^3). Direct comparison of lesion volume evaluated at 7 T versus 3 T revealed that lesion volume on 7 T MRI scans was overestimated of about 13.8% (median value).

No patient was diagnosed with an associated venous malformation on routine MRI scans. On the SWI 3 T scans 3 patients were diagnosed with an associated venous malformation. Five additional patients with associated venous malformations were found on 7 T SWI scans. Thus, 8 patients were diagnosed with an associated DVA that have not been detected on routine MRI scans (p<0.01). Among the subgroup of 11 surgical patients, two patients were diagnosed with associated DVA on 7 T scans which was also proven during surgery (Fig. 3). Consecutively, the absence of associated DVAs as diagnosed at 7 T MRI was also proven intraoperatively in the remaining nine patients. In order to illustrate the above mentioned data two case reports are presented in Figs. 2 and 3 (see figure legends for detailed information).

4. Discussion

Already in 1997 the first article on susceptibility weighted imaging had been published. Still, SWI has yet to be included into routine clinical neuroimaging protocols for CCMs. The necessity of longer echo-times for opposed phase conditions and higher spatial resolution led to seriously long acquisition times at low field strength with lower signal to noise ratio and increased motion artefacts (Dammann et al., 2010; Reichenbach et al., 1997). With the availability of high and ultra-high field strength conditions improved for susceptibility weighted imaging. Initial data suggest that ultra-high-field magnetic resonance imaging at 7 T improves the detection of cerebral cavernous malformations when compared to 1.5 T (Dammann et al., 2010; Novak et al., 2003; Schlamann et al., 2010). Still, there is an ongoing discussion in the pertinent literature if the increased sensitivity of CCM detection reported by previous authors is due to high field strength per se or to SWI sequences since for some data lesion prevalence has been evaluated at high field using SW imaging and at lower field using GRE sequences (Campbell et al., 2010; Schlamann et al., 2010). So far a systematic study comparing SWI sequences at 3 T and 7 T protocols has not been described.

Our study clearly demonstrates that using SWI at 7 T has a higher sensitivity for the detection of CCMs and associated DVA detection
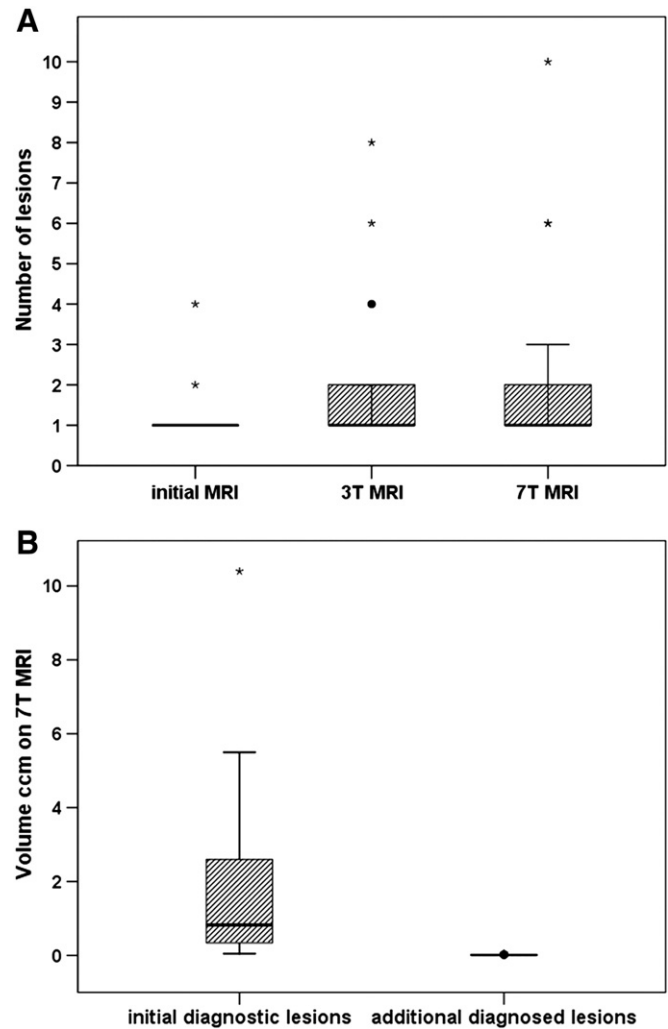
Fig. 1. In Fig. 1A the number of lesions on the different available MRI scans is depicted. Patients presented with a heterogeneous group of initial diagnostic MRIs thus leading to the radiological diagnosis of CCM. Initially only 2 patients were diagnosed with multiple lesions. After study inclusion and informed consent standardised SWI and T1 scans on 3 T and 7 T were performed and evaluated. Significantly more lesions were detected on SWI at 7 T compared to 3 T scans, thus leading to the diagnosis of 6 additional patients with multiple lesions. Fig. 1B compares the volume of diagnosed CCMs. The volume of the initial diagnosed lesion on 3 T MRI is compared with the additionally diagnosed CCMs that were diagnosed only on 7 T SWI sequences. It is important to note that the additionally diagnosed CCMs on 7 T SWI sequences are significantly smaller than the CCMs that were also diagnosed on the 3 T sequences. Lesions volume was evaluated on 7 T SWI scans for all lesions. Box plots represent median value (50th percentile) and range. Outliers (values that are between 1.5 and 3 times the interquartile range) are marked with a circle. Extreme values (values that are more than 3 times the interquartile range) are marked with an asterisk. In order to simplify graphic presentation one extreme value of initial diagnostic lesion volume has been cut in Fig. 1B.

compared to SWI at 3 T. Therefore, our results substantially add to initial data and are conducted for the first time in a larger series of CCM patients, with the additional evaluation of associated DVAs.

The detection of until now occult cerebral cavernous malformations may play an important role in the clinical management and diagnosis of drug resistant and cryptogenic seizure patients, as stated before (Schlamann et al., 2010). There is general consensus in the pertinent literature that seizure disorders represent the most frequent clinical symptoms of supratentorial cavernous malformations. Although the cavernous malformation itself presumably does not generate seizures, the epileptic effect on the surrounding tissue is most likely related to hemosiderosis and reactive gliosis, which are caused by recurring micro-haemorrhages into the surrounding brain parenchyma (Bertalanffy et al., 2002; Robinson et al., 1991; Stavrou et al., 2008). The surgical
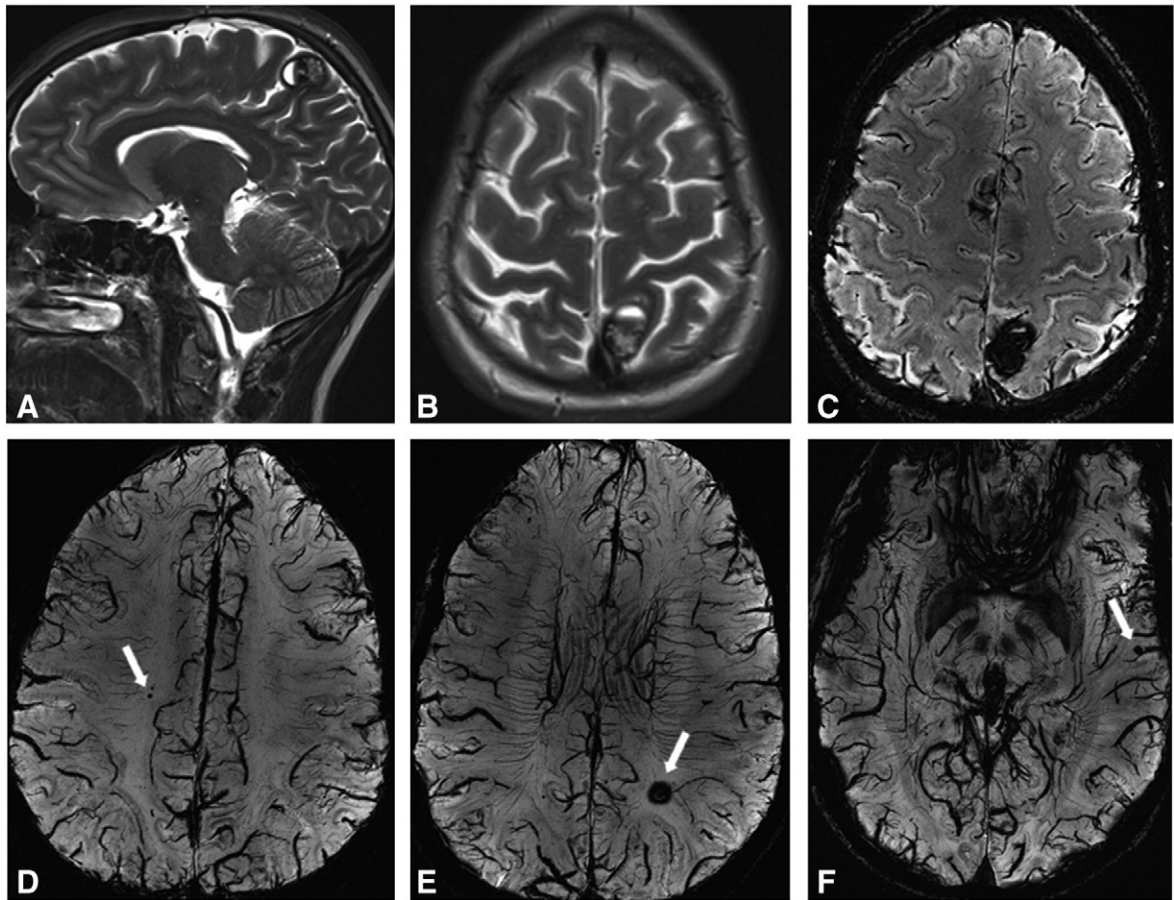
Fig. 2. Fig. 2 depicts pre-operative images of a female patient, 27 years old who initially presented with severe headache and visual disturbances. Consecutively a parietal CCM with haemorrhage could be diagnosed (Fig. 2A, B; 3 T T2) on initial diagnostic T2 images. This lesion could obviously also be identified and 7 T SWI scans (Fig. 2C). However, evaluating the 7 T scans additional 5 lesions could be detected (Fig. 2D–F; 7 T SWI mIP). The parietal lesion was surgically removed and the diagnosis of a CCM was histo-pathologically verified. Retrospectively one of the additional diagnosed lesions (Fig. 2E) could have been detected on the 3 T scans. At 3 months after surgery the patient is free of any neurological symptoms.

excision of the CCM and its surrounding hemosiderin rim has been described as beneficial for seizure treatment in many patient series (Baumann et al., 2007; Bertalanffy et al., 2002; Cappabianca et al., 1997; Stavrou et al., 2008).

Drawbacks and problems of ultra-high-field SWI scans have been discussed previously: especially higher susceptibility artefacts in brain areas close to pneumatised bones such as the skull base as well as overestimation of lesions size of about 11% have been described (Dammann et al., 2010; Schlamann et al., 2010). In the presented study, artefacts severely interfered with the evaluation only in two patients. Still, the overestimation of lesion size has also been noted in our study to a comparable extent. The overestimation of lesion size is based on the increased susceptibility effect of hemosiderin on SWI with the increasing field strength. This effect has to be considered when using

ultra-high-field SWI scans for pre-operative as well as radiosurgical planning and possible implementation into neuronavigation devices. Naturally, this consideration is of paramount importance for deep seated lesions or lesions in other eloquent areas such as the brainstem (Campbell et al., 2010; Dammann et al., 2010; Schlamann et al., 2010).

The association of CCMs and venous malformations and its clinical implications is still controversially discussed. Those developmental venous anomalies are characterised by the occurrence of one or more pathological veins. Porter et al. showed in their series of surgically resected brainstem cavernomas a 100% association with venous malformations. However, only 32% of those DVAs were diagnosed on MRI (Bertalanffy et al., 2002; Porter et al., 1999). Those findings and other studies led to the conclusion that the prevalence of cavernomas associated with DVAs is underestimated using routine MRI and that small venous
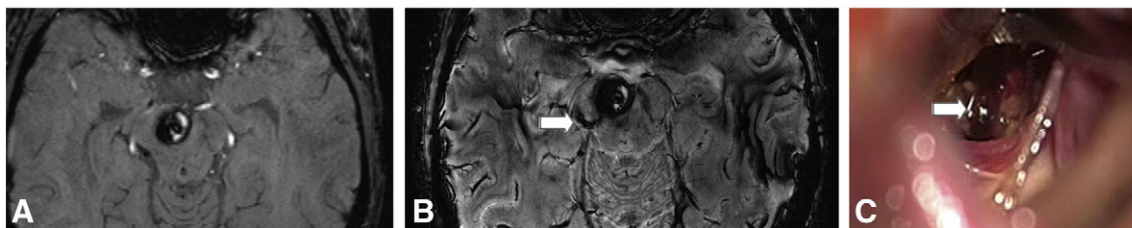
Fig. 3. Depicted are images of a female patient, 27 years old who initially presented with headache and cranial nerve deficits. MRI revealed a CCM in the right cerebral peduncle with intralesional haemorrhage. On the 3 T scan no associated venous malformation was diagnosed (Fig. 3A). In comparison 7 T SWI sequences revealed an associated pathological vein (Fig. 3B arrow) that could also be seen during surgery (Fig. 3C arrow). The diagnosis of a CCM was proven histo-pathologically. Three months after surgery the patient still suffers from a partial paresis of the right oculomotor nerve.

malformations are diagnosed only during surgery. In our series no associated venous malformations were diagnosed on the initial routine MRI thus adding to previously published data (Bertalanffy et al., 2002; Kamezawa et al., 2005; Porter et al., 1999; Wurm et al., 2007). One explanation regarding this circumstance is that if CCM lesions are intact and have not bled, they may be almost invisible except for a faint or ill-defined non-specific blush of enhancement after contrast administration. In addition, the lack of flow-related signal intensity makes CCMs undetectable on conventional MR angiographic techniques. On the other hand DVAs are mainly detected on images after contrast enhancement (Bertalanffy et al., 2002; Tsui et al., 2009).

However, the accurate pre-operative diagnosis of DVAs is essential since it has been described that cavernomas with associated developmental venous anomalies present with a higher risk of clinically significant haemorrhages (Bertalanffy et al., 2002; Porter et al., 1999; Wurm et al., 2007). Therefore, it is important to find a diagnostic sequence for the accurate detection of both CCMs and associated DVAs. In the patient series of Pinker et al. no associated DVA could be detected on 3 T SWI scans (Pinker et al., 2007). In our series DVAs could be detected with SWI at 3 T but to a higher number with SWI at 7 T. Importantly, we could verify our results in our subgroup of surgical resected patients thus confirming the 7 T data with 100% accuracy. 7 T SWI scans seem to enable the detection of CCMs and associated DVAs without the administration of contrast enhancement. It is tempting to speculate that the administration of contrast enhancement at 7 T might further increase the detection rate of associated venous malformations since the resolution at 7 T is improved. However, preliminary data in brain tumours have shown that gadolinium contrast enhancement was similar between field strengths (Lupo et al., 2011; Moenninghoff et al., 2010).

One drawback of the study is of course the verification of observations at ultra-high-field 7 T MRI. As it has been described before, this is a problem of every new method (Schlamann et al., 2010). Other reasons for hypointense lesions on SWI images have to be taken into account. However, as described above, SWI sequences are highly sensitive to paramagnetic blood degradation products such as hemosiderin. What is seen in the diagnosis of CCMs on SWI is the hemosiderin rim in larger cavernous malformations or the hemosiderin due to micro-haemorrhage in smaller lesions. As a differential diagnosis calcifications or micro-angiopathic haemorrhages are possible although they are not common among young and otherwise healthy patients as presented in this study (Blitstein and Tung, 2007; Dammann et al., 2010; Haacke et al., 2009).

In conclusion susceptibility weighted imaging at 7 T improves the diagnosis of cerebral cavernous malformations and associated venous malformations and substantially adds to clinical and pre-operative information. Further, with the use of 7 T imaging it will be possible to gain new insights into lesion dynamics via long term follow up of conservatively and radio-surgically treated patients.

References

Baumann, C.R., Acciarri, N., Bertalanffy, H., Devinsky, O., Elger, C.E., Lo, R.G., Cossu, M., Sure, U., Singh, A., Stefan, H., Hammen, T., Georgiadis, D., Baumgartner, R.W., Andermann, F., Siegel, A.M., 2007. Seizure outcome after resection of supratentorial cavernous malformations: a study of 168 patients. Epilepsia 48, 559–563.

Bertalanffy, H., Benes, L., Miyazawa, T., Alberti, O., Siegel, A.M., Sure, U., 2002. Cerebral cavernomas in the adult. Review of the literature and analysis of 72 surgically treated patients. Neurosurgical Review 25, 1–53.

Blitstein, M.K., Tung, G.A., 2007. MRI of cerebral microhemorrhages. AJR. American Journal of Roentgenology 189, 720–725.

Campbell, P.G., Jabbour, P., Yadla, S., Awad, I.A., 2010. Emerging clinical imaging techniques for cerebral cavernous malformations: a systematic review. Neurosurgical Focus 29, E6.

Cappabianca, P., Alfieri, A., Maiuri, F., Mariniello, G., Cirillo, S., de Divitiis, E., 1997. Supratentorial cavernous malformations and epilepsy: seizure outcome after lesionectomy on a series of 35 patients. Clinical Neurology and Neurosurgery 99, 179–183.

Dammann, P., Barth, M., Zhu, Y., Maderwald, S., Schlamann, M., Ladd, M.E., Sure, U., 2010. Susceptibility weighted magnetic resonance imaging of cerebral cavernous malformations: prospects, drawbacks, and first experience at ultra-high field strength (7-Tesla) magnetic resonance imaging. Neurosurgical Focus 29, E5.

Frischer, J.M., Pipp, I., Stavrou, I., Trattnig, S., Hainfellner, J.A., Knosp, E., 2008. Cerebral cavernous malformations: congruency of histopathological features with the current clinical definition. Journal of Neurology, Neurosurgery, and Psychiatry 79, 783–788.

Haacke, E.M., Xu, Y., Cheng, Y.C., Reichenbach, J.R., 2004. Susceptibility weighted imaging (SWI). Magnetic Resonance in Medicine 52, 612–618.

Haacke, E.M., Mittal, S., Wu, Z., Neelavalli, J., Cheng, Y.C., 2009. Susceptibility-weighted imaging: technical aspects and clinical applications, part 1. AJNR. American Journal of Neuroradiology 30, 19–30.

Kamezawa, T., Hamada, J., Niiro, M., Kai, Y., Ishimaru, K., Kuratsu, J., 2005. Clinical implications of associated venous drainage in patients with cavernous malformation. Journal of Neurosurgery 102, 24–28.

Ladd, M.E., 2007. High-field-strength magnetic resonance: potential and limits. Topics in Magnetic Resonance Imaging 18, 139–152.

Lupo, J.M., Li, Y., Hess, C.P., Nelson, S.J., 2011. Advances in ultra-high field MRI for the clinical management of patients with brain tumors. Current Opinion in Neurology 24, 605–615.

Mittal, S., Wu, Z., Neelavalli, J., Haacke, E.M., 2009. Susceptibility-weighted imaging: technical aspects and clinical applications, part 2. AJNR. American Journal of Neuroradiology 30, 232–252.

Moenninghoff, C., Maderwald, S., Theysohn, J.M., Kraff, O., Ladd, M.E., El Hindy, N., van de Nes, J., Forsting, M., Wanke, I., 2010. Imaging of adult astrocytic brain tumours with 7 T MRI: preliminary results. European Radiology 20, 704–713.

Novak, V., Chowdhary, A., Abduljalil, A., Novak, P., Chakeres, D., 2003. Venous cavernoma at 8 Tesla MRI. Magnetic Resonance Imaging 21, 1087–1089.

Pantano, P., Caramia, F., Bozzao, L., Dieler, C., von Kummer, R., 1999. Delayed increase in infarct volume after cerebral ischemia: correlations with thrombolytic treatment and clinical outcome. Stroke 30, 502–507.

Pinker, K., Stavrou, I., Szomolanyi, P., Hoeftberger, R., Weber, M., Stadlbauer, A., Noebauer-Huhmann, I.M., Knosp, E., Trattnig, S., 2007. Improved preoperative evaluation of cerebral cavernomas by high-field, high-resolution susceptibility-weighted magnetic resonance imaging at 3 Tesla: comparison with standard (1.5 T) magnetic resonance imaging and correlation with histopathological findings—preliminary result. Investigative Radiology 42, 346–351.

Porter, R.W., Detwiler, P.W., Spetzler, R.F., Lawton, M.T., Baskin, J.J., Derksen, P.T., Zabramski, J.M., 1999. Cavernous malformations of the brainstem: experience with 100 patients. Journal of Neurosurgery 90, 50–58.

Raychaudhuri, R., Batjer, H.H., Awad, I.A., 2005. Intracranial cavernous angioma: a practical review of clinical and biological aspects. Surgical Neurology 63, 319–328.

Reichenbach, J.R., Venkatesan, R., Schillinger, D.J., Kido, D.K., Haacke, E.M., 1997. Small vessels in the human brain: MR venography with deoxyhemoglobin as an intrinsic contrast agent. Radiology 204, 272–277.

Robinson, J.R., Awad, I.A., Little, J.R., 1991. Natural history of the cavernous angioma. Journal of Neurosurgery 75, 709–714.

Schlamann, M., Maderwald, S., Becker, W., Kraff, O., Theysohn, J.M., Mueller, O., Sure, U., Wanke, I., Ladd, M.E., Forsting, M., Schaefer, L., Gizewski, E.R., 2010. Cerebral cavernous hemangiomas at 7 Tesla: initial experience. Academic Radiology 17, 3–6.

Stavrou, I., Baumgartner, C., Frischer, J.M., Trattnig, S., Knosp, E., 2008. Long-term seizure control after resection of supratentorial cavernomas: a retrospective single-center study in 53 patients. Neurosurgery 63, 888–896.

Tsui, Y.K., Tsai, F.Y., Hasso, A.N., Greensite, F., Nguyen, B.V., 2009. Susceptibility-weighted imaging for differential diagnosis of cerebral vascular pathology: a pictorial review. Journal of the Neurological Sciences 287, 7–16.

Wurm, G., Schnizer, M., Fellner, F.A., 2007. Cerebral cavernous malformations associated with venous anomalies: surgical considerations. Neurosurgery 61, 390–404.